Solidification of viscous melts: the interplay between nanoscale physics and macroscopic behaviour

J. Bechhoefer

Dept. of Physics
Simon Fraser University
Burnaby, British Columbia, V5A 1S6, Canada
E-mail: johnb@sfu.ca

Abstract: As the undercooling of a liquid melt is increased, one observes several qualitatively different regimes of solidification, each dominated by a different set of physics. I discuss the different regimes, their phenomenology, their physics, and the transitions between them. The experimental focus is on soft-condensed-matter systems, whose widely variable time scales allow one to easily explore the different solidification regimes. One challenge is to relate the complicated nanostructures that are observed to the relatively simple overall macroscopic behaviour.

Keywords: solidification; dendritic growth; banded spherulites; phase-field models; morphology transitions; atomic force microscopy.

Reference to this paper should be made as follows: Bechhoefer, J., 'Solidification of viscous melts: the interplay of nano- and macroscopic phenomena', *Int. J. Nanotechnology*, Vol. x, No. x, pp.xxx–xxx.

Biographical notes: John Bechhoefer received his Ph. D. in Physics from the University of Chicago and was a postdoctoral fellow at the Université de Paris–Sud (Orsay) and the Ecole Normale Supérieure de Lyon before joining the Physics Department at Simon Fraser University in 1991. His research interests range from soft matter (solidification and pattern formation) to biophysics (DNA replication, applications of scanning probe microscopy) to technology (control theory).

1 Introduction

The process of freezing a viscous melt has been a subject of long-standing investigation in many fields, combining elements of condensed matter physics, materials science, and physical chemistry. Although many industrial processes such as casting use temperature quenches to induce solidification, it is better for scientific purposes to impose a more controlled environment. Typically, a liquid melt is held in a container whose boundaries are set to a temperature that is below the solid-liquid coexistence temperature of the melt. The difference $\Delta T \equiv T_0 - T_\infty$ is called

Copyright © 200x Inderscience Enterprises Ltd.

the undercooling, where T_0 is the solid-liquid coexistence temperature and T_∞ the temperature of the boundaries. After the liquid melt is cooled to the container temperature T_∞, one nucleates a solid germ in the bulk, either by introducing a seed crystal or by waiting for a large enough thermal fluctuation. The phase transformation process then transforms the entire sample into a crystalline or amorphous solid (Fig. 1).

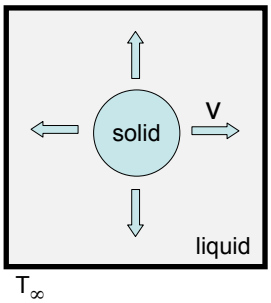

Figure 1 Schematic of free growth of a solid into a fluid. The boundaries of the fluid container are held at a temperature T_∞, implying an undercooling $\Delta T = T_0 - T_\infty$, with T_0 the solid-liquid coexistence temperature. The overall solid-liquid interface grows at a velocity v, which depends on the undercooling.

One can usually classify the experimentally observed behaviour into different regimes, as a function of undercooling ΔT.

- At equilibrium ($\Delta T = 0$), solid and liquid coexist. In principle, the surface tension of the solid-liquid interface, which varies with respect to the underlying crystal lattice, will determine the shape of the crystal [1]. In practice, surface forces often are rendered irrelevant by large kinetic barriers, and the shape is determined by the growth history prior to setting $\Delta T = 0$ [2]. But whether in equilibrium one or not, observed shapes are a mixture of facets, missing orientations (cusps), and smoothly rounded surfaces.

- At moderate undercoolings, the growth is often diffusion limited. The growth of a pure material releases latent heat at the solid-liquid front. After the front reheats to equilibrium, any excess heat must be transported away before any further growth. In the diffusion-limited regime, the growth rate is limited by the rate of heat conduction away from the interface. The typical experimental phenomenon is an instability of the growing solid-liquid interface shape that leads to snowflakes [3], dendrites [4], and other patterns.

- At larger undercoolings – the focus of this article – the experimental phenomena are completely different: instead of a single crystal with a complicated boundary shape, one observes a multicrystalline aggregate with a spherical boundary, known as a spherulite. In contrast to the situation with diffusion-limited growth, the dominant physical processes are much less well understood.

- Finally, at very large undercoolings, the liquid is often trapped in a metastable, glassy state. Although the transition to a glassy state and the properties of that state are topics beyond the scope of this brief review, the subject is still being actively investigated [5].

In this article, we first briefly review the physics of diffusion-limited growth in order to contrast and put into perspective the physics of that well-understood case with that of the more poorly understood spherulitic growth, which is characteristic of intermediate undercoolings. We focus in particular on our work on a commonly seen instability known as banded spherulitic growth. Experimentally, one encounters spherulites in a broad range of materials, ranging from minerals and metals to polymers to liquid crystals to organic molecules. Because solidification velocities decrease in viscous liquids, these phenomena have most often been studied in systems with viscous melts, and the examples we discuss below all fall into that class. As we shall see, one of the main challenges in understanding spherulitic growth and its variants lies in relating the complicated nanostructure to the collective, macroscopic behaviour. The atomic force microscope has turned out to be a powerful tool for exploring the nanostructure. We end with a discussion of various mechanisms that have been proposed to explain banded growth.

In exploring the various regimes of solidification, we focus on the case of a pure material. It is important to note that similar phenomena are also seen in mixtures. In that case, besides temperature, there are additional control parameters – concentration, and chemical potential (set by vapour pressure, e.g., by relative humidity). As an example, precipitates of L-ascorbic acid dissolved in methanol show behaviours similar to those discussed below (single crystal, dendrite, spherulitic growth, banding) as a function of concentration and relative humidity [6].

2 Diffusion-limited solidification

Diffusion-limited solidification has been intensively investigated over the last thirty years and by now is well understood, at least in the non-faceted case [7, 8, 9]. The regime is one where the growth rate of the solid-liquid interface is limited by the diffusion of excess latent heat away from the solid-liquid interface. (For a binary mixture or an impure material, growth is usually limited by mass diffusion.) Qualitatively, we can understand how the growth rate is limited by diffusion as follows: As the material freezes, it releases a latent heat L. If that heat were contained within the volume in which it was released, it raise the temperature by L/c_p, where c_p is the heat capacity. As this temperature rise can often exceed the undercooling (in water, it is $\approx 80°\mathrm{C}$), the front will stop freezing until the excess latent heat is transported away from the interface. Part of the heat remains near the interface (whose temperature thus rises to the coexistence temperature), while the rest must be removed. In the simplest case, the transport will be by thermal diffusion. (In more complicated cases, fluid convection or radiative transport will also help remove heat from the interface.)

Two approaches to modeling have been widely used to describe diffusion-limited growth. The first uses 'sharp-interface models.' This is the traditional approach, where each bulk phase (solid and liquid) and interface (solid-liquid) is described as a separate thermodynamic entity. The second uses 'phase-field models.' In this more recent approach, one introduces an auxiliary, spatially varying field that takes one value in the solid and another in the liquid. The field is continuous, and the solid-liquid interface has a finite thickness. We describe both approaches briefly.

2.1 Sharp-interface models

From linear, non-equilibrium thermodynamics, one can derive a minimal model of diffusion-limited growth [10]:

$$D\nabla^2 T = \partial_t T \ , \tag{1}$$

$$T(\vec{\varphi}) = T_0 \left(1 - d_0 \kappa[\vec{\varphi}]\right) \ , \tag{2}$$

$$L\frac{d\vec{\varphi}}{dt} \cdot \hat{n} = Dc_p \left[\vec{\nabla} T\Big|_{\rm Solid} - \vec{\nabla} T\Big|_{\rm Liquid} \right] \cdot \hat{n} \ . \tag{3}$$

Here, $\vec{\varphi}$ is the position of the solid-liquid front, D is the thermal diffusivity, $\hat{n}$ is a unit vector perpendicular to the interface, and κ is the local interface curvature. The thermal conductivities and densities of both phases are assumed to be equal, for simplicity. Equation 1 describes thermal diffusion in the two phases (solid and liquid). Equation 2 describes the correction to the equilibrium coexistence temperature T_0 due to the local curvature $\kappa[\vec{\varphi}]$ of the front. The capillary length d_0 is a microscopic length given by γ/L, where γ is the solid-liquid surface tension, assumed isotropic here for simplicity. Equation 3 reflects energy conservation: the latent heat released at the interface is conducted away into the liquid and solid phases.

The diffusion of excess heat from the interface leads to an interface shape instability known as the Mullins-Sekerka instability [11]. Schematically, as shown in Fig. 2, a protrusion on a flat interface compresses locally the isotherms in front of the moving interface. This locally larger temperature gradient implies enhanced heat flow away from the interface and, hence, more rapid growth. Thus, bumps become more pronounced, sharpening until rounded off by surface tension (via the Gibbs-Thomson effect). These two effects combine to give a basic length scale for dendrites, which is the geometric mean between a macroscopic diffusion length (D/v, where v is the front velocity) and the microscopic capillary length, d_0.

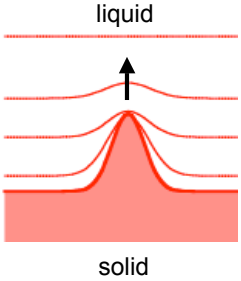

Figure 2 Sketch illustrating the Mullins-Sekerka instability. The thick line is the solid-liquid interface. Thin lines are isotherms of the diffusing latent heat field. Note how the isotherms are compressed in front of a protrusion. Because the heat current away from the protrusion is larger, it grows faster, creating an instability.

The solution to Eqs. 1–3 is a recent feat of applied mathematics [7, 8, 9]. In the equations of motion, surface tension is a numerically weak effect, and early analyses attempted to treat it as a regular perturbation. But since the surface tension coefficient multiplies the highest derivative term (the curvature), it is a singular perturbation and must be treated by a kind of nonlinear generalization of

WKB techniques [7, 8, 9]. In the end, a plausible case has been made that one can account for the fractal-like shapes of dendrites (including tip shape and sidebranch frequency) and for the observed solidification velocities. The strong influence of the surface-tension term explains how small anisotropies in the surface tension can nonetheless create large effects on the macroscopic shape. Thus, we now understand how the hexagonal symmetry of ice leads to the six branches of a typical snowflake – a scenario first posed by Kepler in 1611 [12].

Sharp-interface models may seem a natural way to model solidification, and they have led to significant analytical progress. The major strength of such methods is that one can focus on the shape of a two-dimensional interface rather than the full three-dimensional heat or concentration field. This feature becomes a disadvantage when confronted with more complex morphologies such as multiple domains of fully dendritic growth that coalesce. (This happens when a material is frozen by casting). In such cases, the complexity of the solid-liquid interface shape defies analytic solution. Numerically, progress is also difficult, as Eqs. 1–3 define a 'free-boundary' problem where the interface (and all the meshing associated with the numerical solution) must constantly be displaced and adapted as the front moves.

2.2 Phase-field models

Phase-field models are an alternate way of modeling solidification that is initially more complex but ultimately allows easier numerical exploration of complex situations [13, 14]. One introduces a new variable, a *phase field*, $\phi(\vec{x}, t)$, that is essentially a non-conserved order parameter. By convention, $\phi = 0$ in the liquid phase and 1 in the solid phase. The liquid-solid interface has finite thickness, with ϕ smoothly varying between 0 and 1. Physically, the order parameter can be associated with one of the components of the Fourier series expansion of the density. (Taking just one coefficient amounts to assuming an isotropic surface tension; anisotropy can arise when several order parameters are considered simultaneously.) In the liquid, the density is uniform and the finite-wavenumber coefficients are zero; hence $\phi = 0$. In the solid, the order parameters take on finite values, and hence so does ϕ.

We consider a minimal phase-field model for a pure substance with equal materials properties in both phases [14]. Let $u \equiv (T - T_0)/(L/c_p)$ be the dimensionless local undercooling. Then

$$\tau \frac{\partial \phi}{\partial t} = \xi^2 \nabla^2 \phi - \frac{\partial f}{\partial \phi} \,, \tag{4}$$

$$\frac{\partial u}{\partial t} = D \nabla^2 u + \frac{\partial \phi}{\partial t} \,, \tag{5}$$

where the length ξ sets the scale of the interface thickness (typically a nanometer, or less). The free energy $f(\phi, u)$ is given by a double-well potential in ϕ. The two wells have equal free energy at the solid-liquid coexistence ($u = 0$) and tilt one way or the other as the temperature varies. The form of the potential is somewhat arbitrary (and not too important as long as general features such as a double-well are present); a common choice is

$$f(\phi, u) = W \phi^2 (1 - \phi^2) + L p(\phi) u \,, \tag{6}$$

where the minimum corresponding to the liquid is at $\phi = 0$ and that of the solid at $\phi = 1$. The parameter W sets the height of the energy barrier separating the two phases (and is related to the surface tension), while L is the latent heat. As written, W and L are scaled by an energy chosen so that the time τ in Eq. 4 corresponds to the order-parameter relaxation scale. The 'interpolating function' $p(\phi)$ increases monotonically from 0 to 1 as ϕ goes from liquid to solid values. (The obvious choice $p = \phi$ is inconvenient because it does not keep the liquid and solid phases at $\phi = 0$ and 1 for all undercoolings.) In Eq. 5, the ϕ term describes the release of latent heat. In Eq. 6, the last term describes how the released latent heat affects the degree of order in Eq. 4 (e.g., modeling how released heat can melt the solid).

Now let us consider solving Eqs. 4–6. Compared to the sharp-interface equations, there are two fields (temperature and order-parameter), rather than one, and they are coupled. The advantage, though, is that the equations are solved on a single domain, of simple geometry (the liquid container). The sharp-interface equations, by contrast, must be solved on a domain bounded by a solid-liquid interface that can change not only its shape but also its topology (as domains coalesce, etc.). One can show that the phase-field model contains all of the physics of the shape interface model (e.g., the Gibbs-Thomson effect relating the curvature of the solid-liquid interface to a shift in coexistence temperature) [14]. Indeed, it also contains non-equilibrium, kinetic effects (which can be added to sharp-interface models but are not in the simplified one presented above).

One difficulty with phase field models is the wide disparity between the interface-thickness scale ξ (nanometers) and the scale of the diffusion fields (microns to millimeters). There is a corresponding disparity between the microscopic relaxation time τ (picoseconds) to the times required to form structures (seconds to minutes). In principle, a numerical simulation should span the full range of length and time scales present, a seemingly impossible task. Recently, though, Karma and colleagues have shown that by cleverly scaling dimensional variables, one can relate the results of simulations done at relatively large microscopic length and time scales to parameters that match experimental situations [15, 16]. The microscopic parameters must still be small compared to the macroscopic variations, but the range of scales needed for the simulation is drastically reduced.

Besides being able to represent situations where the interface shape is extremely complex, phase-field models also allow one to include other types of physics by straightforward extension. Thus, one can include a large surface tension anisotropy to study the effects of faceting (both equilibrium and non-equilibrium) [17]. One can include the effects of multiple grains, each with its own crystal orientation. One can also include convective flow in the fluid [14]. Such flexibility will be important when considering growth farther from equilibrium, below.

3 Spherulitic growth

In the diffusion-limited regime, there is a clear distinction between the nucleation of a domain and its growth. No matter how complicated a snowflake or dendrite's shape may become, the underlying crystal lattice is (ideally) a single crystal. In the spherulitic regime, this is no longer true. One does observe what appear to be the isolated nucleation of distinct objects ("spherulites"), but when

one investigates the crystal structure of these objects, they are seen to be polycrystalline, not monocrystalline. As discussed above, spherulitic growth is seen in almost all classes of materials (including metals, minerals, polymers, organics, liquid crystals, and biological molecules) [18, 19]. The main requirement is the ability to crystallize at relatively large undercoolings; often the melt is relatively viscous, too. There are many variants of spherulitic growth, but all are polycrystalline, with at least approximate radial symmetry, as illustrated in Fig. 3. (The figures in this section are all examples of spherulitic growth that are also banded. We discuss the banding aspects in the next section.)

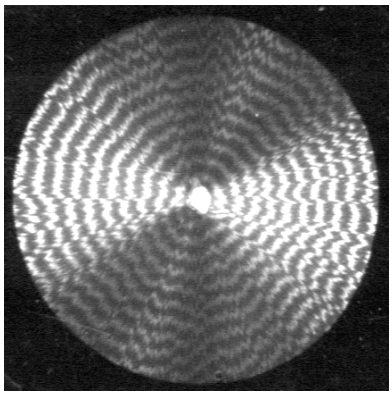

Figure 3 Optical microscope image of ethylene-carbonate — 6.56 wt.% polyacrylonitrile spherulite growing into the melt at an undercooling $\Delta T = 8.6$ °C. Reflected light illumination, with the azimuthal contrast coming from the angle between source and the radial fibres. Band spacing is 750 μm. (Image by J. Kirkby.)

In the spherulitic regime, diffusive transport plays at most a minor role in the growth. Diffusion-limited growth is affected by boundary conditions once the front is within a few diffusion lengths (D/v) of the container. A snowflake grown in a square box will have an overall square shape once its diffusion field begins to interact with the boundary. By constrast, spherulite growth in small droplets shows no effect on such length scales [20]. Further, in very thin samples, much of the latent heat is effectively conducted away into the sample substrate with little observable effect, other than a possible shift in the temperature at the front [21, 22]. In the simplest case, the sample is thin enough and growth slow enough that one may regard the solidification as isothermal. Finally, while the chemical-segregation effects that control the growth of alloys are present also in spherulites, they do not play a controlling role, as may be noted by varying alloy (or impurity) concentration. In particular, spherulitic growth is present even in very pure materials [23, 20].

What then limits the growth for spherulites? A general answer is attachment kinetics [24, 25]: the moving solid-liquid interface is a wave of ordering that sweeps through the material, causing adjacent liquid molecules to find their ordered position against the growing solid phase. The time to perform this attachment can set the front velocity for a given temperature. The attachment event may be as simple as a molecule that finds its proper place in the growing solid plane or it may require adopting a complex internal configuration. If there is faceting, the attachment is more rapid on steps, as the multiple bonds increase the binding energy to the surface. Such steps will be present if there are screw dislocations or if a terrace (with

its edges) has nucleated. By contrast, an atomically flat plane has no steps, which hinders attachment.

Another relevant factor concerns the transport of molecules to the interface. The solid phase is typically $\approx 10\%$ denser than the liquid phase, meaning that liquid molecules must be brought in from ever longer distances to pack into the solid. In a viscous fluid, this transport time can limit the growth velocity [26].

Why do spherulites show an overall radial order with non-crystallographically orientations? One of the most detailed analyses of spherulite structure has been done on spherulites in elemental selenium, a metal where molecules in the liquid spontaneously form chains of 'living polymers'. Bisault et al. [23] give evidence for a regular structure whose dominant motif is the presence of repeated small-angle-branching events, which cause local crystallites to be rotated with respect to each other by a few degrees. They also conclude that the small-angle branching is not due either to twinning or to tip-splitting of the growing crystal face. To get a feel for how such processes might work, one can look at the core region of a spherulite, which often has a 'sheaf-of-wheat' texture [Fig. 4(a)]. The standard view of this is that the spherulite starts initially from a single needle, from which new needles branch [23]. The repeated small-angle branches eventually close in among themselves, creating a defect line and two cavities, and also lead to an approximately radial ordering of the outer branches. In our work on banded spherulites, we see similar ordering about the core (Fig. 4). Figure 4(c) illustrates how growth as highly anisotropic needles, coupled with small-angle branching, can start to produce a symmetric shape. Recently, the groups of Chan and Li have shown this process in real time by AFM by studying slowly freezing spherulites [27].

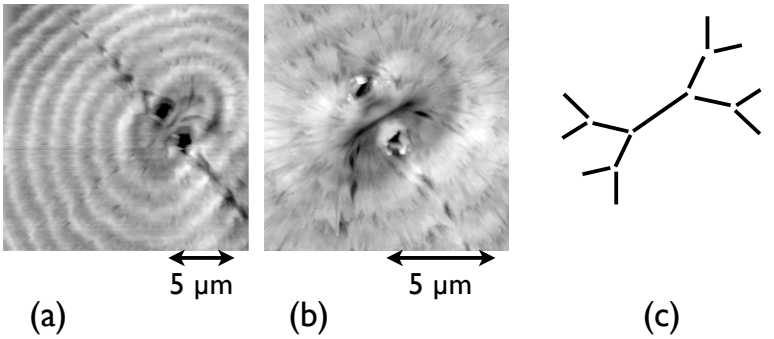

Figure 4 Optical (a) and AFM (b) micrographs of 10OCB spherulite nuclei with sheaf structures. (c) Illustration of the growth of the initial lamellae. Adapted from [20].

Although the existence of small-angle branching is well-documented, its origins are less clear. Possibilities that have been suggested are that surface-tension imbalances on the different faces of crystallites can bend or rotate them [28, 29] and that the fluid flow induced by the density difference between solid and liquid phases leads to what is essentially channel flow between growing crystallites [26]. The higher pressure present between the tips can be sufficient to splay the fibers, if they are long (and hence floppy) enough. (For polymers, Bassett[30] has suggested that the splaying of nearby crystallites may be due to the steric interaction of nearby dangling chains. Such an explanation, of course, would not be relevant for small-molecule spherulites, such as those formed in liquid crystals [20].)

3.1 Theoretical approaches to spherulitic growth

For many years, work on spherulitic growth has been primarily experimental, and much of that work (e.g., [18]) has been qualitative, with little reference to detailed theory. Most of the sustained theoretical effort has been to develop theories of polymer crystallization that focus on the homogenous nucleation and subsequent growth of individual lamellae. These works have historically concentrated on understanding what distinguishes polymer crystallization from that of small molecules. For example, a celebrated observation by Keller in the 1950s was that polymers crystallized in narrow lamellae with folded chains whose longitudinal axis is normal to the growth direction [31], and many theories have focused on this aspect (e.g., on what sets the thickness of the lamellae) [32, 33]. Much more detailed simulations of 'ideal' polymers can now be done on computer, and recent studies are injecting a number of new ideas into the field (e.g., the sharing of polymer strands among several nuclei [34] and the role of metastable phases [33, 35]).

The work on polymer crystallization cited above also consider spherulitic growth. But because such theories put in so many details specific to polymers (chain entanglement, reptation, etc.), it becomes difficult to understand the general features of spherulitic growth common to polymeric and non-polymeric materials. Another approach is to search for a minimal model that can generate the range of observed phenomena. From this point of view, the recent paper by Gránásy et al., which generalizes the phase-field model of Sec. 2.2 to describe spherulitic growth, is a major advance [36].

Gránásy et al. focus on isothermal growth of a two-component alloy, which in effect amounts to replacing the undercooling field u by a concentration field c. (The free energy is slightly more complicated, including the contributions from the solution energy and the entropy of mixing.) The important new feature is an field θ that is strongly coupled to the order field ϕ. In the solid phase, the value of θ gives the orientation of the local crystal. An anisotropy is included that has local minima at $\theta = 0$ (which favors extended domains of a single orientation) and $\theta = \theta_0$ (which favours domain boundaries at a preferred angle θ_0). In the liquid phase, the orientation field fluctuates randomly in space with a correlation length of microscopic dimension, reflecting the *local* orientation order in liquids. A second important feature is the addition of noise terms for all three fields, which allows for nucleation of new domains.

The 'minimal' model of Gránásy et al., while complicated (and requiring the equivalent of 40 CPU years of 2-GHz processor power for their study!) is the first model that can generate essentially the entire range of observed types of spherulitic growth merely by changing the simulation parameters of a single model. The crucial parameters turn out to be the ratio of rotational to translational diffusion constants and the above-mentioned attachment anisotropy. Both slow rotational diffusion and the formation of grain boundaries with finite misorientation can lead to non-crystallographic branching. The former is more relevant for highly viscous melts, the latter for pure materials at relatively low undercoolings. In both cases, secondary nucleation takes place continually at the growing front and leads to a growth envelope that has a spherical envelope. This confirms the picture of small-angle branching and non-crystallographic branching discussed above but does not entirely explain the origin of the branching. (The anisotropy term, while plausible,

is essentially put in by hand.) Nonetheless, the correspondence between simulation and experiment is impressive. While the study remains qualitative in that the thickness of interfaces is larger than for actual materials, it shows that very simple mechanisms are at the heart of some of the main observations of spherulitic growth. There is also nothing in principle that prevents more detailed modeling with parameters that correspond better to real materials. The only obstacle at present is the long computations required. The tricks involving asymptotics pioneeered by Karma et al. [15] (Sec. 2.2) may prove useful here, too.

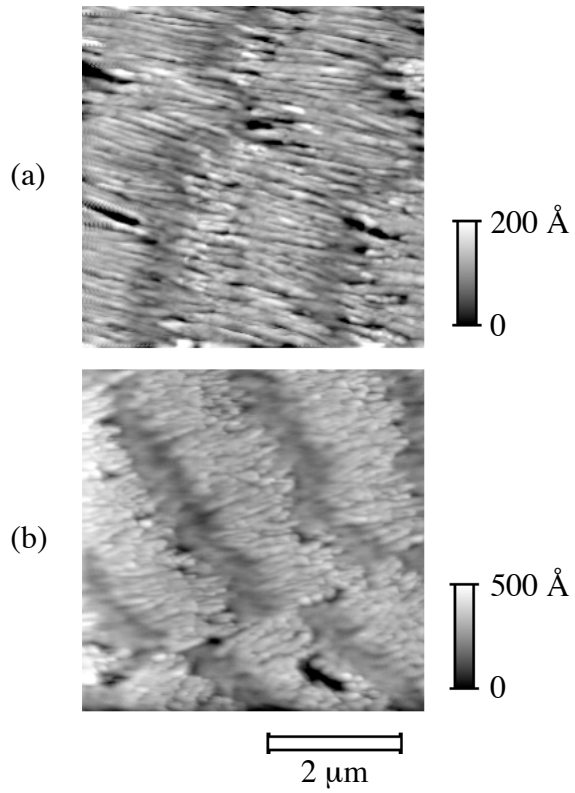

Figure 5 Atomic-force micrographs of spherulitic bands of the liquid crystal 10OCB. The samples were grown between glass plates, which were subsequently separated. The bands are composed of radially oriented needles with lengths on the order of the band spacing. (a) Spherulite grown at ΔT=25 °C. (b) Spherulite grown at ΔT=32 °C. Note the sharp change in band phase. From [20].

4 Banded spherulites

Banded spherulites are a common variant of spherulitic growth, occurring either throughout the spherulitic regime or at the large-undercooling part of it. Like other spherulites, banding is observed in a wide range of materials, including polymers [37], liquid crystals [20], selenium [23], organics [38], and minerals [39]. A variety of observations suggests that the periodic bands are associated with a radial twist

of crystalline axes as one goes out from the centre of the banded domain. Techniques used include polarizing microscopy, electron microscopy, microbeam X-ray diffraction, and micro-Raman spectroscopy [40, 41]. As for the rotation itself, it has been hypothesized to be caused by either a twisting of individual crystallites (with a ribbon-like shape) or a statistical rotation of independent crystallites. Electron microscope or AFM images, for example Fig. 5a, are generally inconclusive, as the nanostructure is complex.

The work of my group has focused on the studies of banded spherulites in unusual materials such as liquid crystals and small organic molecules mixed with a small amount of polymer. The study of non-polymeric banded spherulites actually predates that of polymeric systems. Already in 1929 (before polymers were understood to be long molecules!), Bernauer published a detailed study of over 200 materials, including many observations that were later repeated in polymeric systems [38]. Even so, the study of such systems has lagged behind that of polymers, and much less is known about them.

Our first set of studies concerned the liquid crystal 10OCB, which exhibits spherulitic growth when the smectic A phase (playing the role of a viscous liquid) freezes into a crystalline phase [42, 43, 20]. Unlike polymeric molecules, 10OCB is short, with a rigid core and short, flexible tail. The materials used are relatively pure, and adding small amounts of impurities does not change the behaviour. Key observations were that as the undercooling increased, the solidification morphology made a series of distinct transitions (dynamical analogies of phase transitions), in contrast to previously postulated continuous crossovers [42, 43]. In studies of the properties of the banded spherulite regime itself [20], AFM images vividly confirmed that growth is not limited by a diffusion field in the spherulitic regime. Optical micoscope images such as Fig. 3 often show bands with abrupt phase shifts, associated with different dynamical domains (analogous to different domains in a polycrystal). In Fig. 5b, we see that the discontinuity between such domains occurs essentially between two individual crystallites – it is sharp even on the nanoscale!

AFM images have also yielded interesting observations about the structure of the nucleation site. In Fig. 6, we see an example where the inner structure is actually a spiral. Such structures have been seen in other non-equilibrium systems undergoing heterogeneous nucleation (i.e., nucleation on an 'impurity'). Here, the impurity may simply be central domains whose orientation favours growth out of the plane of the (thin) sample. Growth is limited by the sample thickness, but the grains can still serve as sites for the secondary nucleation of the 'correct' orientation of crystallites. Since such nucleation occurs at one point on the boundary of the core, the growth then spirals around the nucleation centre.

In another set of investigations, we looked at systems consisting of small organic molecules mixed with a low concentration of polymer. The polymer is segregated in the liquid phase and serves mainly to increase the liquid's viscosity and thereby slow down nucleation and growth time scales. Such non-polymeric spherulites have parameters characterizing the growth that can be quite different from polymers. In polymers, band spacings are typically 1–100 μm, while in the maleic- anhydride–poly-acrylonitrile system, they are as large as 10 cm [44, 45]. In addition, polymer spherulites often grow at μm/min while the maleic-anhydride system grows at about 10 cm/sec. Because such scales are so large, they are inconvenient to work with, and we have instead focused on a system with intermediate scales: ethylene carbonate

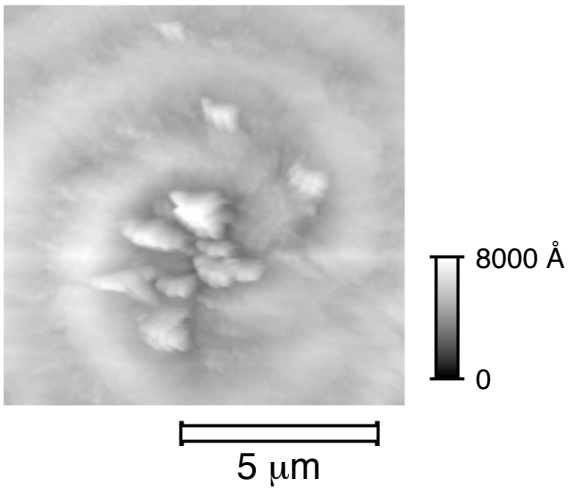

Figure 6 AFM micrograph of spherulite nucleus with a spiral structure. From [20].

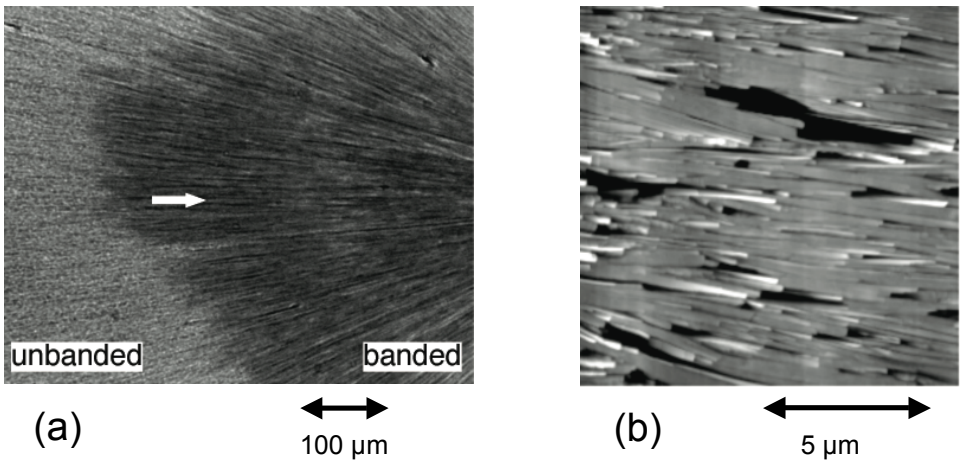

Figure 7 (a) Optical microscope image of transformation of banded spherulites into a more stable structure. (b) AFM image of the transformed, unbanded state. [20].

mixed with small amounts of polyacrylonitrile. In this system, the polymer has a reasonable solubility range, giving a second control parameter in addition to the undercooling [21].

Theoretical discussions of banded spherulitic growth have been controversial and inconclusive. The same forces implicated in the splaying of crystallites in unbanded spherulites have also been hypothesized to play a role in causing the rotation of crystallite axes. A recent review by Lotz and Cheng [37] has vigorously argued the case for surface-stress imbalances on the different faces of crystallites as supplying the mechanical force behind the twist (an argument made earlier by Keith and

Padden [29]). While surface force imbalances no doubt exist, it is less obvious to know whether they are in fact the dominant driving force. Owen has given a simple argument that the twisting produced by surface-stress imbalances should vary as $\Delta T^{-3/2}$. We have carefully measured the divergence in the ethylene-carbonate–polyacrylonitrile system and found, instead, that the transition is analogous to a second-order transition, with a banding wavelength diverging as $(\Delta T - \Delta T_c)^{-\nu}$, with $\nu \approx 1$ and ΔT_c a finite undercooling threshold. The exponent differs from the predicted value and the divergence takes place at finite, not zero undercooling. (See Fig. 8.) (Almost all systems showing banding instabilities show greatly increasing banding wavelengths at low undercoolings; however, in general these systems have not been studied carefully enough to evaluate the divergence behaviour.)

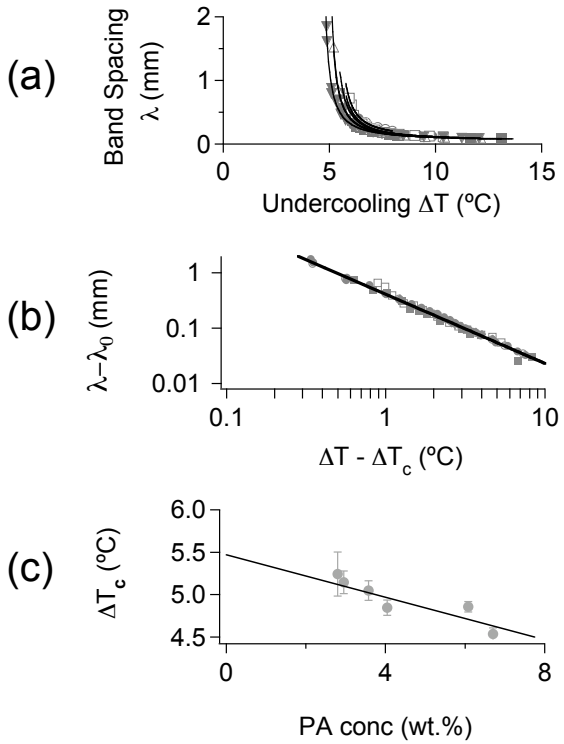

Figure 8 (a) Transition from unbanded to banded spherulitic growth. (Ethylene carbonate with added polyacrylonitrile.) (b) Wavelength divergence near the transition temperature. (c) Dependence of critical undercooling on polymer concentration. From [21].

An old idea – just recently put to rest – is that giant screw dislocations supply the required twisting forces [46, 47]. Recent AFM observations of real-time growth by Xu et al., however, show that (at least in their system) twisting happens first. Screw dislocations are then introduced as a result of the twisting, in order to relieve internal stresses [48].

A variety of more speculative ideas have also been put forth. Schultz [49] argues that crystals may twist in order to reach areas of lower concentration of some growth-limiting diffusion field, an idea inspired by the diffusion-limited growth discussed in Sec. 2. This field need not be the concentration of impurities but could

also be local stresses generated, for example, by the density difference between solid and liquid. This last suggestion recalls an idea of Tiller and Geering, who used hydrodynamic flows generated by the solid-liquid density difference to account for the splay of spherulites [50, 26]. In unpublished work, we have investigated this 'hydrodynamic scenario' in the context of a fiber growing in the mean field of other growing crystallites. The hydrodynamic interaction can cause the growing fibers to bend or twist – whether these forces dominate is again remains unclear.

5 Conclusion

In this article, we have discussed recent observations on banded spherulitic growth and have made a particular effort to place that work in the broader context of classifying the general behaviour of solids crystallizing from the melt at different undercoolings. Unlike other transitions between different morphologies, banded spherulites show a diverging wavelength as a function of undercooling, indicating a second-order morphology transition (or nearly so). The recent development of AFM techniques that probe the structure and – for slowly changing systems – dynamics of spherulites has led to signficant advances and promises much more in the future. The most notable observations so far have been those that demonstrate the local behaviour of the growth down to the level of individual crystallites [20] and those that rule out screw dislocations as a source for the observed rotation of crystalline axes [48].

On the theoretical front, we have discussed several physical models for the origins of the twist. To some extent, all either disagree with experiment or are too poorly developed to apply to real data. An obvious (but computationally challenging) next step would be to try to create a 'minimal banding model' by extending the phase-field model of Gránásy et al. [36] to three-dimensional simulations incorporating a tendency for crystalline axes to twist with an axis along the growth direction. Such simulations would show whether other physics is needed to enforce a coherent twist (such as hydrodynamic effects). Again, the challenge is both to explain the origins of the twist and its coherence over large domains. One could also determine whether the observed pitch divergence at onset emerges in such a minimal model or whether other ingredients are required.

From the point of view of applications of techniques from nanotechnology (such as high-temperature AFM imaging), the problem of spherulitic growth illustrates both virtues and limitations. The virtues are that techniques that probe the nanoscale can provide insights into structure and dynamics that are not available using more macroscopic probes. The limitations are that, as with many condensed-matter problems, large-scale collective effects play an important role. In the end, progress is made by bringing all available tools to bear [51], in order to provide a unified picture.

Acknowledgments

I thank the many students and postdocs who have contributed greatly to the studies done in my laboratory on spherulitic growth. This review has drawn par-

ticularly on work by Jeff Hutter, Bram Sadlik, and Jason Kirkby, to whom I am grateful. The work was funded by grants from NSERC (Canada).

References and Notes

1 Wortis, M. (1988) 'Equilibrium Crystal Shapes and Interfacial Phase Transitions', in *Chemistry and Physics of Solid Surfaces VII,* Vanselow, R. and Howe, R.F., eds., Berlin, Springer-Verlag, pp.367–405.

2 Sekerka, R.F. (2005) 'Equilibrium and growth shapes of crystals: how do they differ and why should we care?' *Cryst. Res. Technol.*, Vol. 40, pp.291–306.

3 Bentley, W.A. and Humphreys, W.J. (1962) *Snow Crystals*, Dover, New York, NY.

4 Langer, J.S. (1980) 'Instabilities and pattern formation in crystal growth', *Rev. Mod. Phys.*, Vol. 52, pp.1–28.

5 Debenedetti, P.G. and Stillinger, F.H. (2001) 'Supercooled liquids and the glass transition', *Nature*, Vol. 410, pp.259–267.

6 Ito, M., Izui, M., Yamakazi, Y. and Matsushita, M. (2003) 'Morphological diversity in crystal growth of L-ascorbic acid dissolved in methanol', *J. Phys. Soc. Japan*, Vol. 72, pp.1384–1389.

7 Langer, J.S. (1987) 'Lectures in the theory of pattern formation', in *Les Houches, Session XLVI — Le hasard et la matière,* Souletie, J., Vannimenus, J. and Stora, R., eds., Elsevier pp.629–711.

8 Kessler, D.A., Koplik, J. and Levine, H. (1988) 'Pattern selection in fingered growth phenomena', *Adv. Phys.*, Vol. 37, pp.255–339.

9 Pomeau, Y. and Ben Amar, M. (1992) 'Dendritic growth and related topics', in *Solids Far From Equilibrium,* Godrèche, C., ed., Cambridge University Press, Cambridge, pp.365–431.

10 Caroli, B., Caroli, C. and Roulet, B. (1992) 'Instabilities of planar solidification fronts', in Godrèche, C., op. cit., pp.155–296.

11 Mullins, W.W. and Sekerka, R.F. (1963) 'Morphological stability of a particle growing by diffusion or heat flow', *J. Appl. Phys.*, Vol. 34, pp.323–329.

12 Kepler, J. (1611) *The Six-Cornered Snowflake*, ed. and transl. Hardie, C., Clarendon Press, Oxford, 1966.

13 Langer, J.S. (1986) 'Models of pattern formation in first-order phase transitions', in *Directions in Condensed Matter Physics: Memorial Volume in Honor of Shang-keng Ma*, World Scientific Press, Singapore, pp.165–186.

14 Boettinger, W.J., Warren, J.A., Beckermann, C. and Karma, A. (2002) 'Phase-field simulation of solidification', *Ann. Rev. Mater. Res.*, Vol. 32, pp.163–194.

15 Karma, A. and Rappel, W.-J. (1998) 'Quantitative phase-field modeling of dendritic growth in two and three dimensions', *Phys. Rev. E*, Vol. 57, pp.4323–4349.

16 Echebarria, B., Folch, R., Karma, A. and Plapp, M. (2004) 'Quantitative phase-field model of alloy solidification', *Phys. Rev. E*, Vol. 70, 061604, pp.1–22.

17 Debierre, J.-M., Karma, A., Celestini, F. and Guérin, R. (2003) 'Phase-field approach for faceted solidification', *Phys. Rev. E*, Vol. 68, 041604, pp.1–13.

18 Magill, J.H. (2001) 'Spherulites: A personal perspective', *J. Mat. Sci.*, Vol. 36, pp.3143–3164.

19 Krebs, M.R.K, MacPhee, C.E., Miller, A.F., Dunlop, I.E., Dobson, C.M. Donald, A.M. (2004) 'The formation of spherulites by amyloid fibrils of bovine insulin', *Proc. Nat. Acad. Sci*, Vol. 101, pp.14420–14424.

20 Hutter, J.L. and Bechhoefer, J. (2000) 'Banded spherulitic growth in a liquid crystal', *J. Cryst. Gr.*, Vol. 217, pp.332–343.

21 Sadlik, B., Talon, L., Kawka, S., Woods, R. and Bechhoefer, J. (2005) 'Critical behavior of the banded-unbanded spherulite transition in a mixture of ethylene carbonate with polyacrylonitrile', *Phys. Rev. E*, Vol. 71, 061602, pp.1–8.

22 Guan, B.X. and Phillips, P.J. (2005) 'Does isothermal crystallization ever occur?' *Polymer*, Vol. 46, pp.8763–8773.

23 Bisault, J., Ryschenkow, G. and Faivre, G. (1991) 'Spherulitic branching in the crystallization of liquid selenium', *J. Cryst. Growth*, Vol. 110, pp.889–909.

24 Nozières, P. (1991) 'Shape and growth of crystals', in Godrèche, *op. cit.*, pp.1–154.

25 Bechhoefer, J. (1994), in *Spatio-Temporal Patterns in Nonequilibrium Complex Systems*, Santa Fe Institute: Studies in the Sciences of Complexity, Vol. 21, Cladis, P.E. and Palffy-Muhoray, P. eds., Addison-Wesley, Reading, MA, pp.107–122.

26 Tiller, W.A. (1991) *The Science of Crystallization. Vol. 1: Microscopic Interfacial Phenomena; Vol. 2 Macroscopic Phenomena and Defect Formation*, Cambridge University Press, Cambridge.

27 Chan, C.M. and Li., L. (2005) 'Direct observation of the growth of lamellae and spherulites by AFM', *Adv. Poly. Sci.*, Vol. 188, pp.1–41.

28 Calvert, P.D. and Uhlmann, D.R. (1973) 'Surface stresses and crystal twisting in hippuric acid and in polymers', *J. Poly. Sci.*, Vol. 11, pp.457–465.

29 Keith, H.D. and Padden, F.J., Jr. (1996) 'Banding in polyethylene and other spherulites', *Macromolecules*, Vol. 29, pp.7776–7789.

30 Bassett, D.C. (1994) 'Lamellae and their organization in melt-crystallized polymers', *Phil. Trans. Roy. Soc. London*, Vol. A348, pp.29–43.

31 Keller, A. (1957) 'A note on single crystals in polymers – evidence for a folded-chain configuration', *Phil. Mag.*, Vol. 2, pp.1171–1175.

32 Hoffman, J.D. and Miller, R.L. (1997) 'Kinetics of crystallization from the melt and chain folding in polyethylene fractions revisited: theory and experiment', *Polymer*, Vol. 38, pp. 3151–3212.

33 Strobl, G. (2006) 'Crystallization and melting of bulk polymers: New observations, conclusions and a thermodynamic scheme', *Prog. Poly. Sci.*, Vol. 31, pp.398–442.

34 Muthukumar, M. (2005) 'Modeling polymer crystallization', *Adv. Poly. Sci.*, Vol. 191, pp.241–274.

35 Hu, W. and Frenkel, D. (2005) 'Polymer crystallization driven by anisotropic interactions', *Adv. Poly. Sci.*, Vol. 191, pp.1–35.

36 Gránásy, L., Pusztai, T., Tegze, G., Warren, J.A. and Douglas, J.F. (2005) 'Growth and form of spherulites', *Phys. Rev. E*, Vol. 72, 011605, pp.1–15.

37 Lotz, B. and Cheng, S.Z.D. (2005) 'A critical assessment of unbalanced surface stresses as the mechanical origin of twisting and scrolling of polymer crystals', *Polymer*, Vol. 46, pp.577–610.

38 Bernauer, F. (1929) *Gedrillte Kristalle*, Berntraeger, Berlin.

39 Wang, Y.F. and Merino, E. (1990) 'Self-organizational origin of agates: Banding, fiber twisting, composition, and dynamic crystallization model', *Geochim. et Cosmochim. Acta*, Vol. 54, pp.1627–1638.

40 Phillips, P.J. (1993) in *Handbook of Crystal Growth, Vol. 2*, Hurle, D.T.J., ed., Ch. 18, Elsevier, Amsterdam.

41 Phillips, P.J. (1990) 'Polymer Crystals', *Rep. Prog. Phys.*, Vol. 53, pp.549–604.

42 Hutter, J.L. and Bechhoefer, J. (1997) 'Three classes of morphology transitions in the solidification of a liquid crystal', *Phys. Rev. Lett.*, Vol. 79, pp.4022–4025.

43 Hutter, J.L. and Bechhoefer, J. (1999) 'Morphology transitions in diffusion- and kinetics-limited solidification of a liquid crystal', *Phys. Rev. E*, Vol. 59, pp.4342–4352.

44 Lagasse, R.R. (1994) 'Exceptionally large banded spherulites', *J. Cryst. Growth*, Vol. 140, pp.370–380.

45 Degen, M.M., Costanzino, N. and Bechhoefer, J. (2000) 'On the properties of large banded spherulites in a maleic anhydride–polyacrylonitrile mixture', *J. Cryst. Gr.*, Vol. 209, pp.953–962.

46 Eshelby, J.D. (1953) 'Screw dislocations in thin rods', *J. Appl. Phys.*, Vol. 24, pp.176–179.

47 Schultz, J.M. and Kinloch, D.R. (1969) 'Transverse screw dislocations – a source of twist in crystalline polymer ribbons', *Polymer*, Vol. 10, pp.271–278.

48 Xu, J. Guo, B.-H., Zhang, Z.-M., Zhou, J.-J., Jiang, Y., Yan, S., Li, L., Wu, Q., Chen, G.-Q. and Schultz, J.M. (2004) 'Direct AFM observation of crystal twisting and organization in banded spherulites of chiral poly(3-hydroxybutyrate-co-3-hydroxyhexanoate)', *Macromolecules*, Vol. 37, pp.4118–4123.

49 Schultz, J.M. (2003) 'Self-induced field model for crystal twisting in spherulites', *Polymer*, Vol. 44, pp.433–441.

50 Geering, G.T. (1968) *The Role of Dendrites in Spherulitic Crystallization*, Ph.D. Thesis, Stanford University.

51 For a promising optical technique, see Kaminsky, W., Claborn, K. and Kahr, B. (2002) 'Polarimetric imaging of crystals', *Chem. Soc. Rev.*, Vol. 33, pp. 514–525.